Structural and synthetic studies of magnesium and zinc tolylformamidinate complexes

Marcus L. Cole,[a] David J. Evans,[a] Peter C. Junk*[a] and Lance M. Louis[b]

[a] *School of Chemistry, Monash University, P.O. Box 23, Clayton Vic 3800, Australia. E-mail: peter.junk@sci.monash.edu.au*
[b] *Department of Chemistry, James Cook University, Townsville Qld 4811, Australia*

Received (in London, UK) 3rd May 2002, Accepted 14th May 2002
First published as an Advance Article on the web 25th June 2002

The reaction of $MgBu_2$ with 2.0 equivalents of di(*p*-tolyl)formamidine (HFTolP) affords the colourless crystalline bis(formamidinate) species $[Mg(FTolP)_2(thf)_2]$ (**1**), $[Mg(FTolP)_2(dme)]\cdot DME$ (**3**) and $[Mg(FTolP)_2(tmeda)]$ (**4**) in moderate to high yield when conducted in tetrahydrofuran, 1,2-dimethoxyethane and toluene–TMEDA, respectively. Compounds **1**, **3**, **4** and the di(*o*-tolyl)formamidinate (FTolO) complex; $[Mg(FTolO)_2(thf)_2]$ (**2**), synthesised in a manner identical to that employed for the preparation of **1**, have been characterised by spectroscopy (^1H NMR, ^{13}C NMR, FTIR) and single crystal XRD. In the solid state, all four species display monomeric octahedral bis(η^2-formamidinate) metal centres that differ solely on the basis of the steric and structural requirements of both the coordinating solvent donor and the formamidinate. Attempts to prepare analogous zinc complexes *via* the treatment of anhydrous $ZnCl_2$ with 2.0 equivalents of the known complex $[\{Li(FTolP)(Et_2O)\}_2]$, or treatment of HFTolP with 0.5 equivalents of $ZnEt_2$ primarily yielded the novel lithium zincate species $[(\mu_5\text{-}O)Li_2Zn_3\{(p\text{-tolyl})NC(H)N(O)(p\text{-tolyl})\}_6]$ (**5**), which includes a trapped dilithium oxygen unit, and the precedented tetrazinc oxygen cluster $[(\mu_4\text{-}O)Zn_4(FTolP)_6]$ (**6**), respectively. The molecular structures of complexes **1**–**6** are discussed, as are alternative routes to species **6**.

Introduction

The coordination chemistry of ligands based upon the amidinate backbone, $[R^1C(NR^2)_2]^-$ (R^1 = alkyl, aryl, amido or H, R^2 = alkyl, aryl, silyl), involves metallic elements spanning the periodic table.[1,2] The classical perception of amidinate ligands is as precursors to 'lantern-type' binuclear transition metal species, general formula $[M_2(amidinate)_n]^{m+}$, which illustrate the dexterity of donation available to the amidinate subunit.[3] It is this predilection for structural manipulation that sets amidinate ligands apart as ideal ligands for the study of geometric ligand effects[4] and coordination environments[5] upon catalytic activity.[6–8] Modification of these attributes can be achieved with ease *via* the rational exchange of R^1 and R^2, yielding tailored combinations of bite angle, steric encumbrance and electron donor capacity.

Several groups have chosen to exploit the adaptability that amidinates provide, with a recent swathe of reports detailing synthetic and theoretical catalytic study of group 13, particularly aluminium, tris(amidinates).[9–11] This has encouraged further studies of related bimetallic Li/Mg[12] and heavy group 13/14 acetamidinate ($R^1 = CH_3$) and benzamidinate (R^1 = Ph)[13–16] complexes in an effort to exploit an untapped research area. In contrast, structural study of s-block formamidinate chemistry (where R^1 = H) has largely been ignored.

As listed, formamidinate ligands are well suited to forming bridging interactions[3] stabilising the close proximity of metal–metal bonded species. The fascinating magnetic properties of these species, which result from electronic communication between the close-contact metals,[17,18] have been well documented, however, in spite of obvious attempts to make analogous zinc complexes none have been comprehensively reported.[19] Meanwhile, the structural archive contains just one example of a magnesium formamidinate complex; $[\{FPh)Mg(thf)\}_2(\mu\text{-}Cl)_2(\mu\text{-}thf)]$ [FPh = PhNC(H)NPh] (**7**), synthesised *via* the reaction of HFPh with methylmagnesium chloride.[20] As such, the known geometric binding modes for formamidinate ligands in magnesium and zinc systems have not been defined absolutely.

The plethora of known amidinate-transition metal binding motifs, which, in basic terms, comprise (i) η^1-monodentate, where the ligand coordinates with a conventional metal–amide bond, displaying bond lengths that approximate discrete single and double bonds on the NCN backbone, *e.g.* $[Pt\{2,6\text{-}(CH_2NMe_2)_2C_6H_3\}\{FTolP\}]$,[21] (ii) η^2-symmetrical chelation, where the ligand coordinates a central metal with similar M–N and C–N bonds, *e.g.* $[Pt\{(PhNC(Ph)NPh)\}_2]$,[22] (iii) η^2-unsymmetrical chelation, where the ligand coordinates a central metal with non-congruent M–N and C–N bonds, *e.g.* $[Ta(Me)Cl_2\{(C_6H_{11}NC(Me)NC_6H_{11}\}_2]$,[23] (iv) $\mu{:}\eta^2$-bridging amidinate, whereby the ligand bridges two metals as in the 'paddle-wheel'/'lantern-type' complex $[Mo_2\{(PhNC(Ph)\text{-}NPh\}_4]$,[24] encourage the pursuit of similar s-block and group 12 formamidinate chemistry. Preliminary results indicate that this will be an area of rich structural diversity given the molecular structure of $[\{Li(FTolP)(Et_2O)\}_2]$ (**8**), reported by Cotton *et al.* in 1997,[20] which exhibits an unknown mode of formamidinate bonding with respect to those described by transition metal systems. In **8**, the formamidinate ligand coordinates in both an asymmetrical η^2-chelate and an augmentative $\mu_2{:}\eta^1$-bridging fashion. This mode of bonding has been observed once in transition metal triazenide chemistry; in $[Rh_2(\mu_2\text{-}CO)(bipy)(dppe)(TolNNNTol)_2][PF_6]_2$,[25] whilst a similar but entirely symmetrical bridging motif ($\mu_2{:}\eta^2$) has been reported by the groups of Lappert and Arnold for the potassium benzamidinate and guanidinate complexes $[K_2\{(Me_3Si)NC(Ph)NC(Ph)=C(SiMe_3)_2\}_2]$, $[K_2\{(Me_3Si)NC\text{-}(Ph)NC(Ph)=C(H)SiMe_3\}_2\{(2,5\text{-}Me_2Ph)CN\}_2]$ and $[\{K(C_6H_{11}\text{-}NC\{N(SiMe_3)_2\}NC_6H_{11})\}_2]$.[26–28] Furthermore, in a concurrent study, we have systematically investigated the

This journal is © The Royal Society of Chemistry and the Centre National de la Recherche Scientifique 2002

structural chemistry of several ether and amine-adducted lithium, sodium and potassium diarylformamidinate complexes, *e.g.* $[Li(dme)_3][Li_2(FTolP)_3]$.[29] These display extensive structural variety provided entirely by the solvent medium employed and the size and steric imposition of the aryl groups appended, *e.g.* 2,4,6-trimethylphenyl *versus para*-tolyl.

The noted scarcity of group 2 formamidinate species demands that bis(formamidinate) magnesium chemistry be studied, as does the absence of fully characterised zinc complexes.[19] Herein, we report the synthesis and solid-state structures of the first bis(formamidinate) magnesium complexes and the generation of two related zinc species from the inclusion of minute amounts of oxygen/moisture during the attempted preparation of compounds of the type $[Zn(FTolP)_2(solvent)_n]_m$. All complexes are discussed relative to the known catalogue of amidinate or dinitrogen donor species, particularly in terms of molecular structure and, in the case of **6**, known 7-azaindolate synthetic strategies.[30]

Results and discussion

Magnesium complexes

Treatment of HFTolP or HFTolO with half an equivalent of dibutyl magnesium at ambient temperature in the presence of THF affords the complexes $[Mg(FTolP)_2(thf)_2]_n$ (**1**) and $[Mg(FTolO)_2(thf)_2]_n$ (**2**) as colourless crystalline solids in moderate yield (64 and 62%, respectively, see Scheme 1). Compounds **1** and **2** are thermally robust materials (m.p. 205 and 168 °C, respectively), which show no sign of decomposition below 250 °C. Their ^{1}H NMR spectra (d_6-benzene, a non-coordinating solvent thereby precluding further solvation) display resonances consistent with a singular ligand coordination environment, including signals at 8.58 and 8.61 ppm attributable to their respective formamidinate backbone protons, and an equimolar proportion of included tetrahydrofuran (by integration 1 formamidinate:1 THF). As such, the backbone proton resonances of **1** and **2** are significantly shifted from that of the neutral HFTolP ligand (NC(H)N resonance 8.24 ppm, d_6-benzene)[20] and the analogous resonance of **7** (7.81 ppm, also d_6-benzene).[20] Likewise, the ^{13}C NMR spectra of **1** and **2** are consistent with a singular coordination mode for the formamidinate ligands, displaying signals at 161.1 and 163.9 ppm for their respective formamidinate backbone carbons, and are otherwise unremarkable. The IR spectra of both species display the absence of residual N–H stretches around 3300 cm^{-1}, indicating clean deprotonation of the amine group of HFTolP and HFTolO. Correspondingly, the absence of a ^{1}H NMR resonance at *ca.* 12 ppm is indicative of deprotonation (HFTolP NH: 12.28 ppm, d_6-benzene).[20]

The absence of differing formamidinate coordination modes within **1** and **2** is intriguing given a recent report from the group of Winter that indicates, *via* extensive variable temperature NMR studies, that bis(dialkylacetamidinate) and bis(dialkylbenzamidinate) ($R^1 = CH_3$ and Ph, respectively) complexes of magnesium exist in a monomer–dimer equilibrium in aromatic solution (d_8-toluene) providing the alkyl group does not inhibit dimer formation as a consequence of sheer steric bulk, *e.g.* $R^2 = Bu^t$([Mg{Bu^{t}NC(CH$_3$)NBu^t}$_2$] (**9**).[31] However, this report also intimates that bis(amidinate) complexes are formed, on reacting *in situ*-prepared lithioamidinates with magnesium dibromide, without the inclusion of diethyl ether (the preparation medium employed) in their immediate composition. We find this highly unlikely given the data presented herein, the successful isolation of **7** from toluene–hexane solution[20] and the known benzonitrile and THF adducts of bis{di(trimethylsilyl)benzamidinate}-magnesium.[32,33] There are also several reported THF adducts of bis{di(isopropyl)amidinate}magnesium complexes, *e.g.* [Mg{Pr^{i}NC(Ph)NPr^i}$_2$(thf)$_2$] and [Mg{Pr^{i}NC(NPr$^i_2$)NPr^i}$_2$-(thf)].[34] Thus, although we are acutely aware of the facility by which s-block amidinate complexes lose solvent, it must be noted that the structural data provided by Winter *et al.* was generated subsequent to removal of reaction volatiles *in vacuo*. Consequently, in spite of the marginally increased electron donation of an acetamidinate or benzamidinate *vis-à-vis* a formamidinate; we find it surprising that Winter *et al.* failed in their attempts to isolate ether adducts of magnesium bis-amidinates and believe this to be inherent to the synthetic procedures used, rather than the composition of the nascent species. Accordingly, the absence of THF donation in complexes of the form **9** would no doubt increase the likelihood of augmentative bridging magnesium–nitrogen interactions that give rise to the aforementioned alternate amidinate coordination modes, this substantiates their absence in the ^{1}H and ^{13}C NMR spectra of **1** and **2**.

Further to the synthesis of **1** and **2**, and in order to increase the likelihood of augmentative solvent donation, analogous syntheses to that of **1** were conducted in the presence of the coordinating solvents DME (1,2-dimethoxyethane) and TMEDA (*N,N,N′,N′*-tetramethylethylenediamine) (Scheme 2), the latter diluted in toluene. These preparations similarly gave isolable colourless crystalline products that were characterised as $[Mg(FTolP)_2(DME)_2]$ (**3**) and $[Mg(FTolP)_2(tmeda)]$ (**4**). As per the isolated tetrahydrofuran adducts, a singular set of resonances attributable to the FTolP ligands is observed in both ^{1}H and ^{13}C NMR d_6-benzene spectra [NC(H)N H^1 and ^{13}C NMR resonances at 8.94 and 8.55, and 159.0 and 162.1 ppm, respectively), as are resonances assigned to included solvent. Both compounds are thermally robust, **4** significantly more so (**4** decomp. 315 °C, **3** decomp. $>$210 °C) adding credence to the supposition that two distinct structural motifs are described by **3** and **4**. This is also suggested by their differing amine/ether:FTolP ratios. Similarly, neither product displays IR active modes attributable to discrete formamidine N–H bonds.

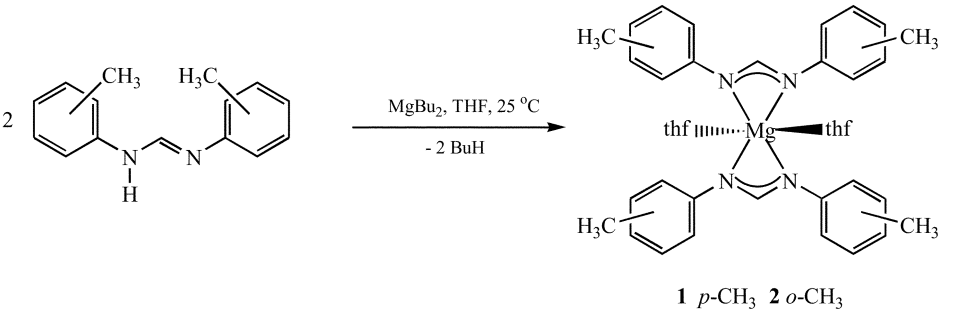

1 *p*-CH$_3$ **2** *o*-CH$_3$

Scheme 1

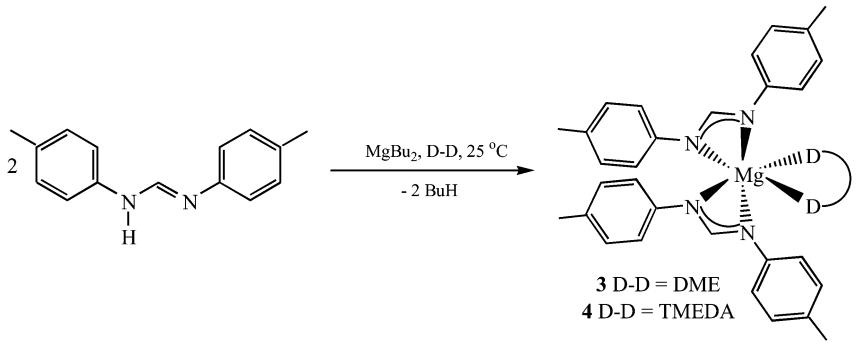

Scheme 2

Table 1 Summary of crystal data for compounds **1**–**6**

	[Mg(FTolP)$_2$-(thf)$_2$] (**1**)	[Mg(FTolO)$_2$-(thf)$_2$] (**2**)	[Mg(FTolP)$_2$-(dme)]·DME (**3**)	[Mg(FTolP)$_2$-(tmeda)] (**4**)	[Li$_2$Zn$_3$O{(*p*-Tol)-NCN(O)(*p*-Tol)}$_6$] (**5**)	[Zn$_4$O(FTolP)$_6$] (**6**)
Mol. formula	$C_{38}H_{46}MgN_4O_2$	$C_{38}H_{46}MgN_4O_2$	$C_{38}H_{50}MgN_4O_4$	$C_{36}H_{46}MgN_6$	$C_{90}H_{90}N_{12}O_7Li_2Zn_3$	$C_{90}H_{90}N_{12}OZn_4$
Mol. weight	615.10	615.10	651.13	587.10	1661.73	1617.22
Temperature/K	296(2)	123(2)	296(2)	296(2)	296(2)	296(2)
Space group	$P2_1/n$	$P\bar{4}2_1/c$	$P2_12_12$	$P2_1/c$	$P\bar{1}$	$Fd\bar{3}$
a/Å	9.5039(6)	13.7728(19)	10.125(9)	13.519(7)	14.9695(17)	28.594(3)
b/Å	16.3981(11)	13.7728(19)	22.47(2)	14.559(8)	16.1059(19)	28.594(3)
c/Å	23.0294(16)	17.9929(36)	8.326(8)	18.815(10)	21.275(3)	28.594(3)
α/°	90	90	90	90	70.803(2)	90
β/°	94.339(2)	90	90	111.055(7)	84.849(2)	90
γ/°	90	90	90	90	88.306(2)	90
Volume/Å^3	3578.8(4)	3413.1(10)	1894(3)	3456(3)	4824.7(10)	26 319
Z	4	4	2	4	2	8
D_c/g cm^{-3}	1.142	1.197	1.142	1.128	1.144	0.919
μ/mm^{-1}	0.087	0.091	0.089	0.084	0.793	0.849
Reflections collected	16 228	12 878	8363	14 959	21 046	26 319
Unique reflections	5137	4221	2707	4973	13 357	1409
R_{int}	0.0645	0.1598	0.1500	0.1738	0.0717	0.2819
Parameters varied	483	207	221	450	1252	84
R_1	0.0563	0.0570	0.0719	0.0887	0.0981	0.0636
wR_2	0.1558	0.0978	0.1549	0.2122	0.2415	0.1462

To establish the participation of the solvent included in compounds **1**–**4**, and assess the solid-state geometries, aggregation and bonding motifs displayed, single crystals suitable for X-ray structure determination were grown from their respective reaction media. Crystallographic data for all four compounds can be found in Table 1, whilst POV-RAY structural illustrations (20% thermal ellipsoids) and relevant bond lengths and angles are presented in Fig. 1–4.

In the solid state, complexes **1**–**4** exist as heavily distorted octahedral six-coordinate monomers without intermolecular contacts. All four species exhibit solely formamidinate ligands that coordinate the central magnesium centre in an η^2-diazaallyl chelate fashion (Fig. 1–4). This coordination is supplemented by the Lewis base donation of the solvent donors. For **1** and **2** this manifests itself as axial tetrahydrofuran coordination [O(1)–Mg(1)–O(2) 176.82(8) and O(1)–Mg(1)–O(1)# 179.74(19)°, respectively] across what is essentially a square planar bis(formamidinate) magnesium [mean nitrogen deviation from planarity; 1.09 (**1**), 0.06° (**2**)] (see Fig. 1 for POV-RAY illustration of **1**, with relevant bond lengths and angles for both **1** and **2**). In contrast, **3** and **4** exist according to the chelate structural preference of the supplementary ligands. In the absence of bridging interactions, which would perhaps make **3** and **4** polymeric, this leads to 'propeller-like' six-coordinate distorted octahedra, the additional DME ligand of **3** being contained within the crystal lattice without interaction with the bis(formamidinate) metal unit of interest, see Fig. 3 and 4.

Compound **1** crystallises in the monoclinic space group $P2_1/n$ with one unique bis-THF magnesium bis(formamidinate) in the asymmetric unit, whilst **2** crystallises in the tetragonal space group $P\bar{4}2_1c$ with half a bis-THF magnesium bis(formamidinate) in the asymmetric unit. The distorted octahedral geometry of both complexes can be explained by the small bite

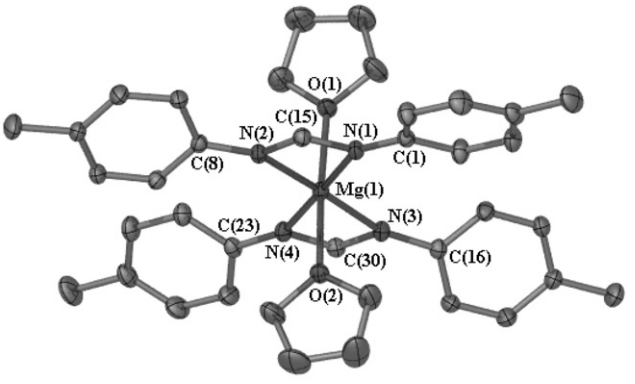

Fig. 1 Molecular structure of [Mg(FTolP)$_2$(thf)$_2$] (**1**), all hydrogen atoms omitted for clarity. Selected bond lengths (Å) and angles (°) for **1**, analogous parameters for **2** in square brackets: Mg(1)–O(1) 2.149(2), Mg(1)–O(2) 2.1510(19) [2.134(2)], Mg(1)–N(1) 2.157(2) [2.158(3)], Mg(1)–N(2) 2.149(2), Mg(1)–N(3) 2.170(2) [2.172(3)], Mg(1)–N(4) 2.150(2), C(15)–N(1) 1.318(3), C(15)–N(2) 1.323(3) [1.321(4)], C(30)–N(3) 1.319(3), C(30)–N(4) 1.312(3) [1.316(4)], N(1)–C(15)–N(2) 116.0(3) [118.3(5)], N(3)–C(30)–N(4) 117.9(3) [119.3(5)], N(1)–Mg(1)–N(2) 62.67(8) [63.43(17)], N(3)–Mg(1)–N(4) 62.88(9) [63.07(16)], O(1)–Mg(1)–O(2) 176.82(8) [179.74(19)], N(1)–Mg(1)–N(3) 118.71(9) [116.75(10)], N(2)–Mg(1)–N(4) 115.72(9) [116.75(10)].

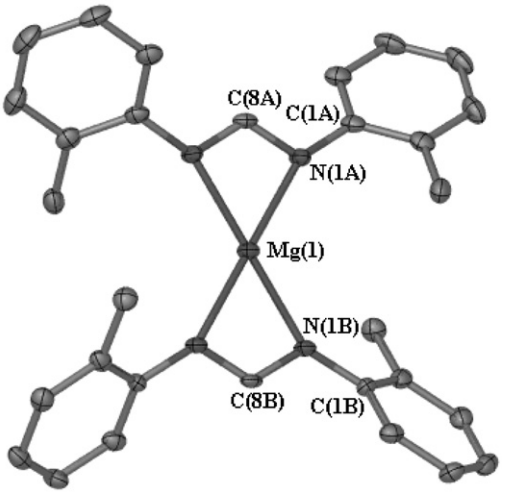

Fig. 2 Molecular structure of $[Mg(FTolO)_2(thf)_2]$ (**2**), depicting twist of tolyl groups. All hydrogen atoms and tetrahydrofuran ligands omitted for clarity. Selected torsion angles (°) for **2**, those of **1** in square brackets: C(1A) ring–C(1A)# ring 79.64(12) [26.83(14)], C(1B) ring–C(1B)# ring 82.80(12) [29.08(16)], N(1A)–C(8A)–N(1A)# to N(1B)–C(8B)–N(1B)# 0.05(4) [4.26(26)].

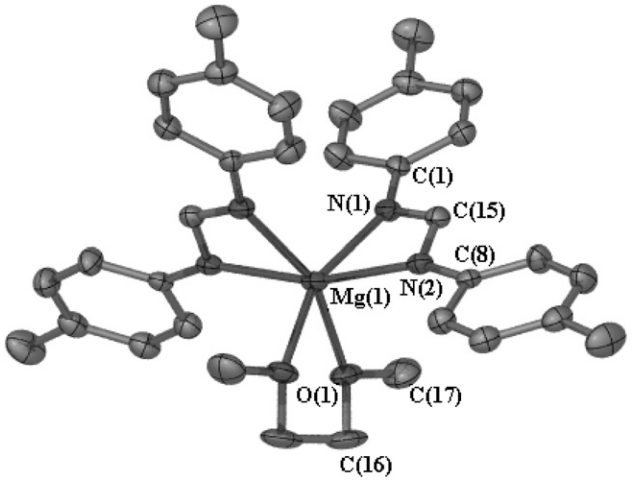

Fig. 3 Molecular structure of $[Mg(FTolP)_2(dme)]\cdot DME$ (**3**), all hydrogen atoms and lattice DME omitted for clarity. Selected bond lengths (Å), torsion angles (°) and bond angles (°): Mg(1)–N(1) 2.121(5), Mg(1)–N(2) 2.140(5), Mg(1)–O(1) 2.133(5), C(15)–N(1) 1.305(7), C(15)–N(2) 1.326(7), N(1)–Mg(1)–N(2) 62.49(19), N(1)–C(15)–N(2) 114.3(6), N(1)–Mg(1)–N(2)# 106.1(2), O(1)–Mg(1)–O(1)# 75.8(3), C(1) ring–C(8) ring 2.42(35), N(1)–C(15)–N(2) to N(1)#–C(15)#–N(2)# 83.80(40).

angle of the formamidinate units. In **1**, these angles are 62.67(8) and 62.88(9)°, whilst in **2** the analogous angles are 63.43(17) and 63.07(16)°. The explanation for this minute opening of the relative N–Mg–N angles is not obvious, but would intuitively lie with the presence of methyl groups in the *ortho*-positions of the aryl rings of **2**, which experience greater steric buttressing than the *para*-methyls of **1**. For **2**, these also bring about a considerable twist of the planes of the phenyl rings relative to one another, the mean torsion angle being 81.22° (see Fig. 2), whilst those of **1** have a mean torsion angle of 27.96°. In any case, these bite angles are typical for s-block complexes of arylformamidinates [64.6(3)° for **8**][20] and slightly constricted with respect to the bite angles of the solvent-free monomeric magnesium bis(amidinate) complex **9** [65.77(7)°],[31] suggesting that the inclusion of tetrahydrofuran donors in the magnesium coordination spheres of **1** and

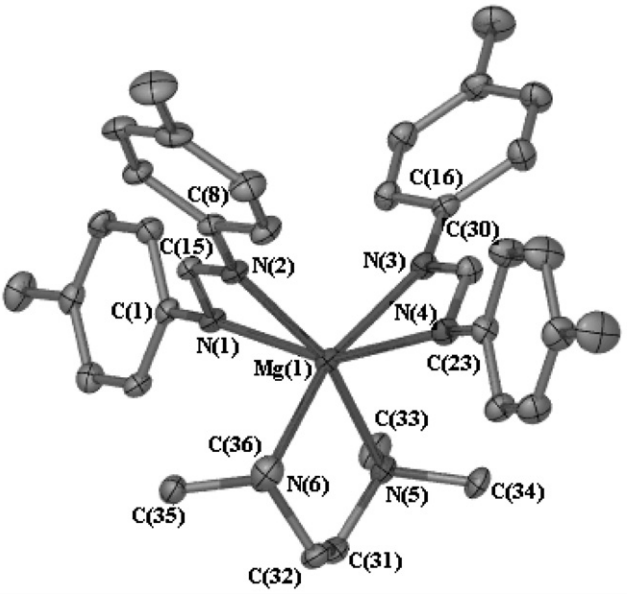

Fig. 4 Molecular structure of $[Mg(FTolP)_2(tmeda)]$ (**4**), all hydrogen atoms omitted for clarity. Selected bond lengths (Å), bond angles (°) and torsion angles (°): Mg(1)–N(1) 2.222(4), Mg(1)–N(2) 2.148(4), Mg(1)–N(3) 2.180(4), Mg(1)–N(4) 2.238(4), Mg(1)–N(5) 2.252(4), Mg(1)–N(6) 2.293(4), N(1)–C(15) 1.319(5), N(2)–C(15) 1.302(5), N(3)–C(30) 1.308(6), N(4)–C(30) 1.329(6), N(1)–Mg(1)–N(2) 61.74(13), N(3)–Mg(1)–N(4) 61.01(15), N(1)–C(15)–N(2) 117.8(4), N(3)–C(30)–N(4) 116.5(4), N(5)–Mg(1)–N(6) 79.59(14), N(1)–Mg(1)–N(3) 99.86(15), N(2)–Mg(1)–N(4) 99.99(15), C(1) ring–C(8) ring 55.12(15), C(16) ring–C(23) ring 47.89(19), N(1)–C(15)–N(2) to N(3)–C(30)–N(4) 85.71(53).

2 incites some steric encumbrance. The magnesium–nitrogen bond lengths of **1** and **2** have a mean average of 2.157 and 2.165 Å, this compares well to the mean structurally authenticated Mg–N amidinate bond of 2.143 Å[35] and the Mg–N bond lengths of **7** (mean 2.133 Å)[20] and **9** (mean 2.042 Å).[31] The extent of delocalisation across the formamidinate backbone can be seen in the comparable C–N bond lengths across both **1** and **2**, these deviate by no more than 0.007 and 0.000 Å, respectively, see Fig. 1, unlike those of HFTolP, which differ by 0.065 Å [discrete single and double C–N bonds of 1.346(6) and 1.281(6) Å, respectively].[20] Furthermore, the mean N–C–N backbone angles of **1** and **2** suggest a considerable progression toward sp^2-hybridisation at the central carbon [117.0 and 118.8°, respectively], again highlighting the structural modification attained by deprotonation of the parent HFTolP and HFTolO [HFTolP N–C–N angle 123.25(8)°].[20] Within the MgN_2C metallocycles of **1** the formamidinate carbons [C(15) and C(30)] protrude 0.003 and 0.031 Å, respectively, above/below the N–Mg–N plane, whilst those of **2** do not as a consequence of the metallocycle lying on a two-fold rotation axis along the C(8A)–Mg(1)–C(8B) vector. This protrusion is perhaps surprising when one considers the considerably less crowded acetamidinate–Mg metallocycles of **9**, *i.e.* no tetrahydrofuran donors, which experience a backbone carbon projection of 0.128 Å above the plane provided by the amidinate N–Mg–N bite.[31] These values serve to confirm that both complexes display solely η^2-diazaallyl binding to the metal centre with no participation of the formamidinate π-system, as would be required in the event of potential Mg–C_{form} interactions. Given the aforementioned deviation from square planarity listed for both transoidal complexes, the sum of their combined formamidinate equatorial plane angles are unsurprisingly 359.98° and 360.00°, whilst the average Mg–O_{THF} for **1** and **2** are 2.150 and 2.134(2) Å, respectively. These are extended compared to the mean average structurally authenticated Mg–O_{THF} bond length of 2.086 Å,[35] and abated

relative to the non-bridging Mg–O_{THF} bonds of dimeric **7** (mean 2.340 Å).[20]

The solid-state structures of species **3** and **4** differ considerably to those of **1** and **2** (see Fig. 3 and 4), although essentially the bonding exhibited is the same. Complex **3** crystallises in the orthorhombic space group $P2_12_12$, with half a solvated magnesium bis(formamidinate) and half a DME of solvation in the asymmetric unit, whilst **4** crystallises in the monoclinic space group $P2_1/c$, with one complete solvated magnesium bis(formamidinate) in the asymmetric unit. As per the η^2-diazaallyl coordination of **1** and **2**, both complexes exhibit near symmetrical chelation, the respective formamidinate backbone C–N bond lengths varying by 0.021 and 0.021 Å, respectively. The magnesium–nitrogen bond lengths of **3** average 2.131 Å, with very little deviation; however, those of **4** are considerably more disparate [Mg(1)–N(2)/N(3) mean 2.164, Mg(1)–N(1)/N(4) mean 2.230 Å]. This appears to result from the proximity of N(1) and N(4) to the TMEDA donor atoms, causing significant interaction of the adjacent *para*-tolyl groups with the bulky NMe_2 groups of the donor. The increase in bulk of the NMe_2 groups over the analogous OMe donors of **3** evidently causes the observed extension of the Mg–N_{form} bond lengths. For comparison, the equivalent deviation in the Mg–N bond lengths of **3** is 0.021 Å.

The pseudo-octahedral geometries of **3** and **4** are distorted to a greater extent than the relatively unperturbed geometries of **1** and **2**. This can be seen in the *cisoid* metal bond angles of both species, these vary in the ranges 62.49(19)–106.1(2) and 61.01(15)–103.51(16)°, respectively, a considerable departure from the ideal of 90° (first angles result from the small formamidinate bite). Likewise, the formamidinate NCN planes exhibit considerable torsion angles to one another [83.80(40) and 85.71(53)°], unlike those of **1** and **2**, which are 4.26(26) and 0.05(4)°, respectively. Akin to **1**, the backbone formamidinate carbons deviate minutely from the N–Mg–N bite planes, 0.036 Å in **3**, and 0.082 and 0.107 Å in **4**, whilst the torsion angles described by the phenyl rings attached to each formamidinate are 2.42(35) (**3**), 55.12(15) and 47.89(19)° (**4**). The discrepancy in these values, *i.e.* **3** relative to **4**, highlights the enhanced steric encumbrance of TMEDA over DME, which incites steric buttressing with adjacent phenyl groups, thereby enforcing a high degree of torsion. Meanwhile, the bite angle described by the chelating solvent donor of **3** [75.8(3)°] is comparable to those found in structures deposited in the Cambridge Structural Database, however, the bite angle in **4** [79.59(14)°] is acute, presumably due to steric crowding (CSD: O_{DME}–Mg–O_{DME} 74.89, N_{TMEDA}–Mg–N_{TMEDA} 81.55°).[35] The mean magnesium–donor atom bond lengths in **3** and **4** are comparable to those in structurally authenticated complexes [2.133(5) (**3**), 2.273 Å (**4**); CCSD Mg–O_{DME} 2.154, Mg–N_{TMEDA} 2.246 Å].[35] Lastly, as per **1** and **2**, both compounds **3** and **4** display formamidinate backbones that suggest a progression to sp^2-hybridisation about the central formamidinate carbon [114.3(6) (**3**) and 117.15° (**4**); mean carbon projection from NNH plane 0.065 (**3**) and 0.038 Å (**4**)]. However, it is interesting to note that the NCN backbone angle of the parent formamidine, HFTolP, is closer to this ideal 120° than the analogous angle of **3** [123.25(8)°].[20]

Zinc complexes

In an attempt to synthesise zinc congeners of complexes **1**–**4**, anhydrous zinc dichloride was treated with two equivalents of the known lithium formamidinate reagent **8**, prepared *in situ* from treatment of the parent formamidine with *n*-butyllithium in diethyl ether (see Scheme 3). This preparation approximates that described within the extensive works of Cotton and coworkers, who utilised the reaction of $[ZnCl_2(HFTolP)_2]$ with 2.0 equivalents of methyllithium to form $[(\mu_4\text{-O})Zn_4\{FPh\}_6]$ after exposure to residual atmospheric moisture.[19] To date, the parent complex, presumably $[Zn_2(FTolP)_4]$ given the aggregation preference of fellow first-row +2 oxidation state transition metal complexes,[3] has not been reported. With this in mind, we undertook the above synthesis.

Upon reaction, a small but persistent amount of precipitate was obtained. In order to assess the identity of this compound, the preparation was repeated without stirring. This resulted in the growth of a small amount of crystalline material, suitable for X-ray structure determination, in low yield (*ca.* 8% by zinc dichloride). A structure analysis revealed the identity of **5**, see Fig. 5, as the lithium zincate complex $[(\mu_5\text{-O})Li_2Zn_3\{(p\text{-Tol})NC(H)N(O)(p\text{-Tol})\}_6]$, which exhibits a bound dilithium oxygen subunit and entirely *N*-oxygenated formamidinates. Oxygen derivatives of amidinates of this type are unknown, but bear a close structural resemblance to alkyl- and benzamid-*N*-alkyloximato ligands ($[RN(O)C(R')=NH]^-$). These display discrete single and double C–N bonds.[36] The absolute origin of the included oxygen is unknown, however, under

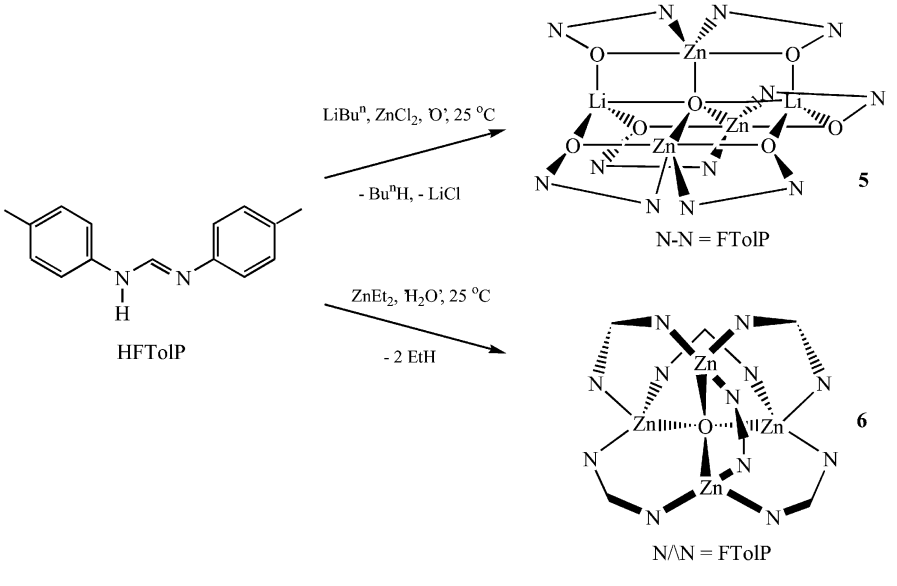

Scheme 3

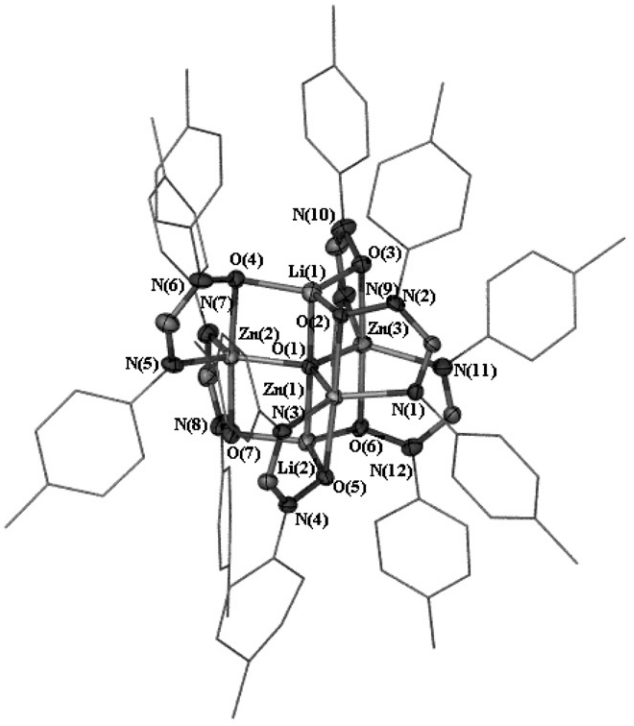

Fig. 5 Molecular structure of $[(\mu_5\text{-O})Li_2Zn_3\{(p\text{-tolyl})NC(H)N(O)(p\text{-tolyl})\}_6]$ (**5**), all hydrogen atoms omitted for clarity. Selected bond lengths (Å) and angles (°): O(1)–Li(1) 1.991(17), O(1)–Li(2) 1.926(19), O(1)–Zn(1) 1.956(6), O(1)–Zn(2) 1.990(6), O(1)–Zn(3) 1.950(6), Li(1)–O(2) 1.926(19), Li(1)–O(3) 1.92(2), Li(1)–O(4) 1.891(19), Li(2)–O(5) 1.93(2), Li(2)–O(6) 1.872(19), Li(2)–O(7) 1.944(18), Zn(1)–N(1) 2.046(7), Zn(1)–N(3) 2.040(8), Zn(2)–N(5) 2.003(9), Zn(2)–N(7) 2.028(9), Zn(3)–N(9) 2.055(9), Zn(3)–N(11) 2.053(9), Li(1)–O(1)–Li(2) 91.9(5), Zn(1)–O(1)–Zn(2) 120.4(3), Zn(1)–O(1)–Zn(3) 91.4(6), Zn(2)–O(1)–Zn(3) 118.6(3), O(2)–Li(1)–O(3) 118.3(10), Li(1)–O(2)–Zn(1) 85.3(5), O(1)–Zn(1)–N(1) 118.5(3), O(1)–Zn(1)–N(3) 122.7(3), N(1)–Zn(1)–N(3) 118.7(3), O(1)–Zn(1)–O(2) 89.5(2), O(2)–Zn(1)–O(5) 1177.8(2), Li(1)–O(2)–N(2) 111.9(8).

the meticulously anaerobic conditions employed, and in view of the syntheses of Wheatley and co-workers (see below),[37,38] we speculate that residual traces of dioxygen accompanying the HFTolP precursor are a likely source. This would perhaps imply that **5** is an intermediate in the aerobic decomposition of a lithium zinc formamidinate complex to lithium and zinc hydroxide (and HFTolP), which incorporates a trapped lithium oxide by-product. Unfortunately, the lack of 'pure' material and considerable insolubility in all common laboratory solvents frustrated all other attempts to characterise complex **5**. It is noteworthy that lithium organozincates have found synthetic utility in organic chemistry,[39] particularly in Michael additions and epoxide ring-opening reactions,[40] however, the structural archives contain relatively few examples of lithium zincate structures.[35] This is of concern, as structural knowledge of bimetallic amido species is fundamental to the modification and tailoring of reagent activity.[41] As such, the molecular structure of complex **5** makes an invaluable contribution should lithium zincate reagents acquire broad application. Thus, in spite of the considerable disorder displayed (limited to modelled disorder about the phenyl ring vectors), the structure determination of **5** is included herein as proof of its novel molecular structure and connectivity. Accordingly, bond lengths and angles are listed, but must be considered tenuous relative to those of compounds **1**–**4** and **6**.

Compound **5**, which crystallises in the triclinic space group $P\bar{1}$, with one molecule of **5** in the asymmetric unit, displays a number of interesting crystallographic features. Like previously reported oxygen-containing zinc formamidinate clusters, *e.g.* $[(\mu_4\text{-O})Zn_4\{FPh\}_6]$,[19] **5** displays a central oxygen atom. However, unlike known oxygenated complexes, including those formed by the sequential reaction of dimethylzinc with 1.0 eq. of diphenylbenzamidine[38] or *N*-methyl/benzyl-2-pyridylamine,[37] *tert*-butyllithium and molecular oxygen recently reported by Wheatley and co-workers, the central oxygen of **5** exists in a trigonal bipyramidal environment, with three equatorial zinc and lithium atoms in the apical positions. This coordination geometry is consistent with the limited number of known μ_5-O hetero- and homometallic species (octahedral being by far the most abundant structural preference),[35] particularly that of $[(\mu_5\text{-O})(\mu_2\text{-Cl})_2(\mu_3\text{-}\{N(CH_2CH_2NSiMe_3)_3\})_2Nd_2Li_3][Li(thf)_4]$[42] which similarly exhibits a heterometallic trigonal equatorial plane. Complex **5** is the first structurally authenticated example of a zinc species that contains $M_1M'_4O$, $M_2M'_3O$ or M_5O polyhedra, discounting those of greater coordination number; $[Bu^t(\mu_3\text{-O})Li_3(\mu_6\text{-O})Zn_3\{N(2\text{-}C_5H_4N)Me\}_6].thf$[38] and $[(\mu_6\text{-O})Li_4Zn_2\{(Ph)NC(Ph)N(Ph)\}_6]$.[37] The entrapment of lithium salts by the lithium amidinate $[Li\{Bu^tNC(Bu^n)NBu^t\}]$ has been addressed in a report by Chivers *et al.*, however, the trapping of lithium oxide was not attempted.[43] Fig. 5 clearly illustrates the geometry of the central oxygen. The tri-zinc equatorial plane deviates from ideal planarity by a mean angle of 0.04°, whilst the oxygen hardly projects above/below the tri-zinc unit (< 0.001 Å). The Li(1)–O(1)–Li(2) axial angle of 178.5(8)° attests to the regular geometry about O(1), whilst the three zinc centres possess similar trigonal bipyramidal geometries that are not appreciably distended by the non-equivalent equatorial atoms [N(3)–Zn(1)–N(1) 118.7(3), O(1)–Zn(1)–N(1) 118.5(3), O(5)–Zn(1)–O(2) 177.8(2)°]. Both lithium centres sit in trigonal pyramidal geometries, the mean O_{form}–Li–$O_{central}$ and O_{form}–Li–O_{form} angles being 94.3 and 119.5°, with an average metallic projection of 0.142 Å above/below the tri-O_{form} plane. Meanwhile the N-oxygenated formamidinates chelate in an η^2-fashion about the zinc atoms, with a bridging oxygen interaction to an apical lithium atom of the central oxygen coordination sphere (see Fig. 5). This provides the formamidinate oxygens with significantly distorted trigonal geometries [Li(1)–O(2)–N(2) 111.9(8), Zn(1)–O(2)–N(2) 107.6(4), Zn(1)–O(2)–Li(1) 85.3(5)°]. Meanwhile, the NCN formamidinate backbones of **5** display disparate C–N bond lengths, *i.e.* near symmetrical and asymmetrical, in the range 0.007–0.070 Å. The combination of these interactions frustrates the inclusion of solvent within the metal coordination spheres of **5**, rendering it solvent/supplementary donor-free in the solid state. The bond lengths in **5**, such as the mean Li–O, Zn–O (both solely FTolP-appended oxygens) and Zn–N lengths of 1.91, 2.157 and 2.038 Å are comparable to the mean of those in structures deposited in the CSD (1.998, 2.063 and 2.098 Å, respectively).[35]

Unfortunately, attempts to isolate the parent complex of compound **5**, *i.e.* the intended zinc bis(formamidinate), proved fruitless, merely yielding intractable solids of low solubility in high polarity solvents and a methylene chloride-soluble material that was later identified as **6** (see below). As such, the reaction of HFTolP with half an equivalent of $ZnEt_2$ was proposed (see Scheme 3), thereby negating the use of lithium reagents and removing the possibility of lithium-zincate species being formed. Accordingly, the HFTolP starting material was rigorously dried *in vacuo* subsequent to repeated recrystallisation from dried and degassed tetrahydrofuran.

Treatment of a tetrahydrofuran solution of HFTolP with $ZnEt_2$ at ambient temperature resulted in the evolution of ethane and formation of a light yellow mother liquor (previously colourless). After stirring for 2 h under a dynamic flow of high purity argon, a significant quantity of colourless precipitate had formed. Cessation of stirring resulted in the deposition of a small quantity of material suitable for XRD study, this revealed the overall bulk precipitate (crystalline sample and precipitate indentical by ^1H NMR in d_1-chloroform) to

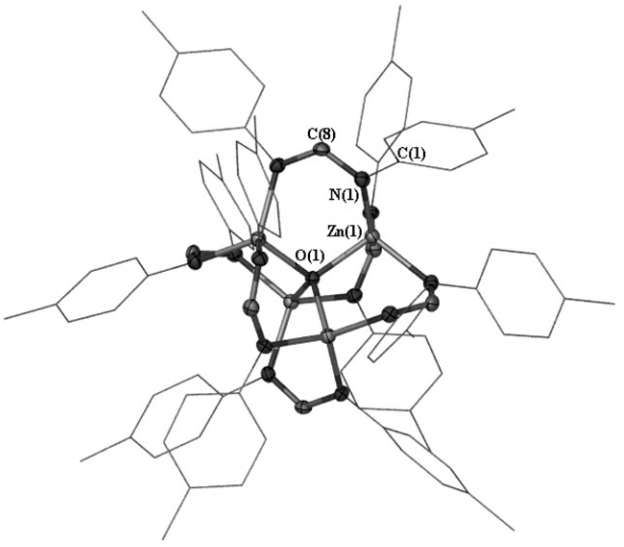

Fig. 6 Molecular structure of $[(\mu_4\text{-O})Zn_4(FTolP)_6]$ (**6**), all hydrogen atoms omitted for clarity. Selected bond lengths (Å) and angles (°): Zn(1)–O(1) 1.9231(15), Zn(1)–N(1) 2.015(6), N(1)–C(8) 1.338(8), Zn(1)–Zn(1)# 3.145(25), Zn(1)–O(1)–Zn(1)# 109.5, N(1)–Zn(1)–N(1)# 113.93(15), N(1)–C(8)–N(1)# 123.1(10), O(1)–Zn(1)–N(1) 104.52(18), Zn(1)–N(1)–C(8) 116.8(6).

be the tetrahedral Zn_4O cluster compound $[(\mu_4\text{-O})Zn_4(FTolP)_6]$ (**6**), which displays solely η^2-bridging FTolP moieties (see Fig. 6). Attempts to isolate the parent compound of **6**, as with **5** before, lamentably resulted in the formation of microcrystalline samples of **6** (by ^{1}H NMR).

Compound **6** is a highly robust solid neither melting nor decomposing prior to 325 °C (limit of apparatus employed). Characterisation of **6** by ^{1}H NMR (d_1-chloroform) indicates two distinct coordination modes for the formamidinate ligands in solution, as the formamidinate *para*-methyl protons consistently resonate as singlets at two separate frequencies of equal integration (2.25 and 2.31 ppm), whilst the aromatic protons appear as two broad multiplets centred at 6.27 and 6.75 ppm. A singular broad resonance attributable to the backbone proton is observed at 7.71 ppm, considerably downfield of that expected for the parent ligand (8.01 ppm, d_6-benzene).[20] Intriguingly, the ^{13}C NMR *para*-methyl signals display no such dichotomy (20.8 ppm, d_1-chloroform), whilst the formamidinate carbons resonate at 166.5 ppm (also d_1-chloroform) and all other resonances appear without similar intensity partner signals. The ^{1}H NMR spectrum (d_6-benzene) of the diphenylformamidinate analogue of **6**, listed above, does not suggest similar differing coordination motifs,[19] however, in the absence of an appended methyl group there is no handle/probe by which to observe such a phenomenon. In view of the molecular structure determination of **6**, which describes perfect T_d symmetry (see below), the origin of the separate ^{1}H NMR signals was not pursued further.

The molecular structure of **6** is displayed in Fig. 6. Unlike the known diphenyl analogue, which was crystallised from toluene–hexane with 1.45 molecules of hexane in the unit cell (space group $P\bar{1}$),[19] **6** crystallises free of solvent (from THF) in the cubic space group $Fd\bar{3}$, with a twelfth of a molecule of **6** in the asymmetric unit. The overall tetrahedral Zn_4O structure is similar to those of basic beryllium and zinc carboxylates,[44–49] essentially consisting of a central oxygen atom (like **5**) in a regular tetrazinc T_d environment [all Zn(1)–O(1)–Zn(1)# 109.5° as necessitated by crystallographic symmetry]. The zinc atoms possess tetrahedral coordination geometries that approach ideality [O(1)–Zn(1)–N(1) 104.52(18), N(1)–Zn1–N(1)# 113.93(15)°] generated by the singular coordination of three distinct bridging formamidinates. These form twisted six-membered OZn_2N_2C metallocycles that are best described as existing in a twisted boat conformation that results from the non-equivalent bond lengths involved; Zn(1)–N(1) 2.015(6), Zn(1)–O(1) 1.9231(15), N(1)–C(8) 1.338(8) Å, the latter being the formamidinate backbone C–N bond that is necessarily symmetrical on the basis of compound **6**'s crystallographic symmetry. These bond lengths compare favourably to the mean bond lengths of the diphenylformamidinate analogue (Zn–N 2.031, Zn–O 1.920, N–C 1.324 Å).[19] The zinc–zinc distance of 3.1406(25) Å displayed by compound **6** is also similar to that of the FPh complex (mean average 3.135 Å).[19] Interestingly, the formamidinate NCN angle of 123.1(10)° is significantly opened relative to those of **2** (mean 118.8°) as a consequence of μ_2:η^2 symmetrical bridging. The geometric regularity of **6** with respect to other first-row analogues, such as the zinc and related cobalt, manganese and iron FPh congeners, is unprecedented. All six OZn_2N_2C metallocycles of **6** are equivalent, whilst the diphenylzinc and cobalt FPh complexes present two distinct sets of 'cycles', providing both M_4O tetrahedra with C_{2v} symmetry.[19] Nonetheless, it must also be recognised that significant disorder was noted in the analogous manganese FPh structure and a different, less symmetrical, bonding motif was exhibited by the iron FPh complex [central oxygen surrounded by two bis(formamidinate) iron moieties near-perpendicularly connected to one another by two separate formamidinates to form a tetrahedral macrostructure].[19] Why there should be any irregularity between the two zinc complexes is a matter of conjecture, although we believe its crystallisation from toluene–hexane and subsequent inclusion of 1.45 molecules of hexane in the asymmetric unit must be culpable.

In view of the dry and meticulously anaerobic conditions employed, the repeated low yield formation of **6** using both zinc halide and alkylzinc preparative methods is perplexing, indicating that the parent complex possesses considerable oxophilicity. Of the known examples of oxo-encapsulation by Zn_n polyhedra, three sources of oxygen can be proposed for species **5** and **6**; (i) atmospheric H_2O,[19,30] (ii) residual dioxygen,[37,38] or (iii) carbon dioxide[49] (although THF-oxygen abstraction has been observed in a lithium-manganese formamidinate system).[50] While the hydrolysis of zinc formamidinate species has precedent for complexes of type **6** (see below),[19,30] the formation of **5** appears to derive from the insertion of oxygen into Li/Zn–N bonds, the archetypal product of hydrolysis being the parent formamidine. Oxygen insertion has been observed for several complexes that derive from the reaction of pre-dried dioxygen with *tert*-butyllithium treated amidozinc alkyls.[37,38] Depending on the amide substituents present, this renders hetero- and homometallic clusters exhibiting encapsulated oxygen, as per **5**. One could surmise that the conditions employed during the attempted preparation that yielded **5** approximate this medium. As an aside, the oxophilicity of the parent species of **6** can be seen in the respective $Zn–O_{central}$ mean bond lengths of complexes **5** and **6**, in that **6** displays relatively smaller bonds (mean 1.965 and 1.9231(15) Å, respectively). This could be considered a moot point given the greater coordination number of the central oxygen of complex **5**, however, both lengths are significantly shorter than the mean structurally characterised Zn–O bond (2.063 Å),[35] indicating substantial metal–oxygen interaction.

On the basis of an NMR scale $ZnEt_2$ preparation of **6** (d_8-tetrahydrofuran–D_2O), we can confirm that the process of conversion from the primary $[\{Zn(FTolP)_2\}_n]$ product to **6** is rapid (< 5 min), concomitantly forming two equivalents of formamidine per molecule of **6**. This complies with the reaction mechanism proposed by Cotton *et al*, shown in Scheme 4, who suggest that the zincate species $[(\mu_4\text{-O})Zn_4(FPh)_6]$ is generated by the reaction of 1.0 equivalent of water with $4/n$ $[\{Zn(FPh)_2\}_n]$ species (solution-state aggregation unknown) yielding two protonated formamidinates.[19] This reaction path

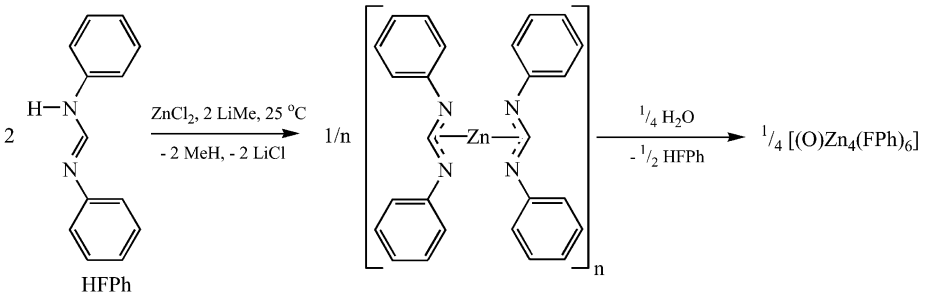

Scheme 4

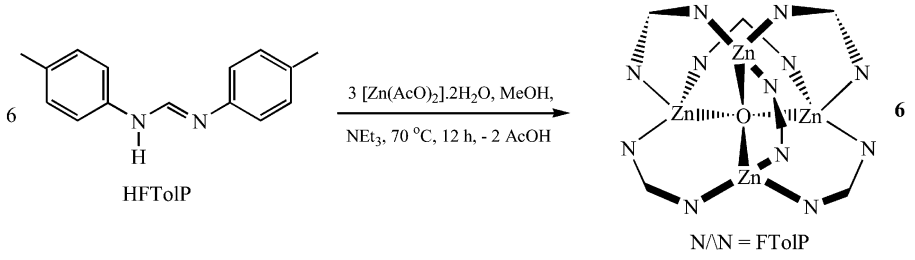

Scheme 5

is facilitated by the absence of readily accessible oxidation states for zinc other than +2, precluding the generation of insoluble oxo and hydroxo species.

Aside from the FPh analogue of **6**, three other anionic dinitrogen donor complexes of the $[Zn_4O]^{6+}$ moiety have been characterised crystallographically. These are the diphenyltriazenate species $[(\mu_4\text{-}O)Zn_4(PhNNNPh)_6]\cdot C_6H_6$,[51] the 2-pyridylbenzylamido complex $[(\mu_4\text{-}O)Zn_4\{N(2\text{–}C_5H_4N)CH_2Ph\}_6]\cdot C_6H_5CH_3$ (alluded to in the *tert*-butyllithium/amidozinc alkyl reactions above)[37] and the 7-azaindolate complex; $[(\mu_4\text{-}O)Zn_4(C_7H_5N_2)_6]$ (**10**),[30] characterised in the solid state with single molecules of methylene chloride and water of crystallisation. The preparation of **10**, in the presence of water, and the overt resemblance of 7-azaindole to an amidine invited the use of a similar methodology in the deliberate synthesis of **6**. To this end, and in-view of the low yield of **6** from rigorously anaerobic routes, six equivalents of HFTolP were reacted with four equivalents of zinc diacetate dihydrate (in the presence of triethylamine) in refluxing methanol (see Scheme 5). This rendered a moderate yield of **6** (52%, identity confirmed by elemental analysis, ^{1}H NMR and unit cell measurement) as colourless prisms after recrystallisation of the reaction precipitate from warm THF. This facile preparation confirms that **6** is both air and moisture stable, offering an alternative path to the study of Zn_4O-amidinate species that circumvents the need for rigorous exclusion of air and moisture in the handling of reactive metal alkyls. We are currently exploiting this simple procedure in order to prepare several analogues of **6** that possess diverse photoluminescent properties borne out of the inclusion of electrophilic and electrophobic groups on the amidinate frame. Our study of these complexes will form the basis of a subsequent publication.

Conclusion

We have shown that the treatment of ditolylformamidines with half an equivalent of $MgBu_2$ renders compounds of the type $[Mg(Form)_2(L)_2]$, where L is a Lewis base donor provided by the solvent medium. In doing so, we have addressed the archival absence of bis(formamidinate) magnesium complexes. For L = tetrahydrofuran, transoidal monomeric octahedral complexes result, the formamidinates inhabiting the equatorial positions and THF donors in the axial positions. For chelating bidentate donors, *i.e.* DME and TMEDA, 'propeller-like' monomeric octahedral complexes result which display forced steric interaction of the tolylformamidinate substituents with adjacent donor groups. This generates distorted six-coordinate magnesium geometries, the degree of deformation depending on donor steric bulk.

Secondly, we have illustrated that the preparation of zinc congeners from the treatment of anhydrous zinc dichloride with lithiated HFTolP primarily yields the unprecedented lithium–zinc–oxygen cluster species **5**, in low yield. Compound **5** possesses solely N-oxygenated formamidinate ligands and a central five-coordinate (trigonal bipyramidal) oxygen, which putatively results from the interaction of an emergent lithium amidozinc species with residual dioxygen. Reaction of diethyl zinc with HFTolP putatively yields a hydrophilic species that, upon hydrolysis, produces the tetrahedral oxygen-centred tetrazinc complex **6**. The facility with which the precursor to **6** undergoes hydrolysis is exceptional given the rigorously air and moisture-free manipulations performed, and goes some way to explaining the archival absence of $[Zn(formamidinate)_2]_n$ species in the structural database.

Lastly, we have demonstrated that complexes of the same type as **6** can be prepared from air-stable precursors, as per known 7-azaindolate strategies, thus negating the need for rigorously anaerobic apparatus, solvents and starting materials.

Experimental

The formamidinate ligand precurors di(*para*-) and di(*ortho*-tolyl)formamidine, HFTolP and HFTolO, respectively, were synthesised according to a published procedure.[20,52] $MgBu_2$, $LiBu^n$, $ZnEt_2$ (1.0, 2.0 and 1.0 M solutions in heptane, pentane and hexanes respectively), $[Zn(acetate)_2]\cdot 2H_2O$ and anhydrous zinc dichloride beads were purchased from Aldrich and used as received. Tetrahydrofuran (THF/thf), 1,2-dimethoxyethane (DME/dme), diethyl ether, toluene and *N,N,N′,N′*-tetramethylethylenediamine (TMEDA/tmeda) were dried over sodium, freshly distilled from sodium–benzophenone or sodium, and freeze-thaw degassed prior to use. Methanol and triethylamine

were used as received (BDH). Dichloromethane was dried and distilled over CaH_2, and freeze-thaw degassed prior to use. All manipulations, except the aerobic method (ii) preparation of complex **6**, were performed using conventional Schlenk or glovebox techniques under an atmosphere of high purity argon or dinitrogen in flame-dried glassware. Infrared spectra were recorded from Nujol mulls using sodium chloride or potassium bromide plates on a Nicolet Nexus FTIR spectrophotometer. ^{1}H NMR spectra were recorded at 300.13 MHz and ^{13}C NMR spectra were recorded at 75.46 MHz using Bruker BZH 300/52 spectrometers with Varian or Bruker consoles and chemical shifts were referenced to the residual ^{1}H or ^{13}C resonances of the solvent used (C_6D_6, $CDCl_3$ or OC_4D_8). Melting points were determined in sealed glass capillaries under argon and are uncorrected. The high aerobic and moisture sensitivity of compounds **1**–**4**, combined with their facile loss of solvent, frustrated the acquisition of meaningful C, H, N microanalytical data.

Syntheses

[Mg(FTolP)$_2$(thf)$_2$] (1). Dibutylmagnesium (2.7 cm^3, 2.7 mmol) was added dropwise to a colourless solution of HFTolP (1.19 g, 5.31 mmol) in THF (50 cm^3), yielding a clear pale yellow reaction mixture that was stirred for *ca.* 2 h. Concentration *in vacuo* and cooling to −30 °C yielded colourless crystals of the title compound (1.04 g, 64%), m.p. 205 °C. ^{1}H NMR (C_6D_6, 300 K): δ 1.31 (m, 8H, CH_2, thf), 2.17 (s, 12H, Ar–CH_3), 3.58 (m, 8H, CH_2O thf), 6.90–7.01 (br m, 16H, Ar-H), 8.61 (s, 2H, NCHN). ^{13}C NMR (C_6D_6, 300 K): δ 21.0 (s, Ar–CH_3), 25.7 (s, CH_2 thf), 68.3 (s, CH_2O thf), 120.1, 123.3, 130.0, 130.8 (s, Ar-C), 161.1 (s, NCHN). IR (Nujol) ν/cm^{-1}: 2360s, 1889m, 1670s, 1503m, 1294s, 1224m, 1173m, 1111m, 1075w, 1038m, 975w, 948w, 922w, 892w, 821s.

[Mg(FTolO)$_2$(thf)$_2$] (2). Dibutylmagnesium (1.0 cm^3, 1.0 mmol) was added dropwise to a colourless solution of HFTolO (0.45 g, 2.01 mmol) in THF (30 cm^3), yielding a clear, colourless reaction mixture that was gently heated and stirred for a period of *ca.* 1.5 h. After heating, a colour change to yellow was observed, whereupon cooling to room temperature yielded a small amount of precipitated product. Filtration and cooloing to −30 °C yielded large colourless prisms of the title compound (0.38 g, 62%), m.p. 168 °C. ^{1}H NMR (C_6D_6, 300 K): δ 1.36 (m, 8H, CH_2, thf), 2.24 (s, 12H, Ar–CH_3), 3.56 (m, 8H, CH_2O thf), 6.97 (m, 8H, Ar-H), 7.01 (d, 8H, Ar-H), 8.58 (s, 2H, NCHN). ^{13}C NMR (C_6D_6, 300 K): δ 21.1 (s, Ar–CH_3), 25.8 (s, CH_2 thf), 69.4 (s, CH_2O thf), 120.0, 121.3, 126.0, 127.5, 129.9, 132.0 (s, Ar-C), 163.9 (s, NCHN). IR (Nujol) ν/cm^{-1}: 2360s, 1674s, 1501m, 1298m, 1172w, 1029w, 881w, 823m, 804m.

[Mg(FTolP)$_2$(dme)]·DME (3). Dibutylmagnesium (1.7 cm^3, 1.7 mmol) was added dropwise to a stirred colourless solution of HFTolP (0.75 g, 3.34 mmol) in DME (40 cm^3), resulting in an exothermic reaction that yielded a clear light yellow reaction mixture. Slight concentration *in vacuo* produced a precipitate, whereupon filtration and storage of the filtrate at −30 °C over 2 h yielded the title compound as fine colourless needles (0.85 g, 78%), m.p. 210 °C (dec). ^{1}H NMR (C_6D_6, 300 K): δ 2.17 (s, 12H, Ar–CH_3), 3.03 (s, 10H, OCH_3 dme and DME), 3.20 (s, 8H, OCH_2 dme and DME), 6.93–7.02 (m, 16H, Ar-H), 8.94 (br s, 2H, NCHN). ^{13}C NMR (C_6D_6, 300 K): δ 21.1 (s, Ar–CH_3), 59.3 (s, OCH_3 dme and DME), 71.2 (s, OCH_2 dme and DME), 119.4, 123.3, 129.7, 130.1 (s, Ar-C), 159.0 (s, NCHN). IR (Nujol) ν/cm^{-1}: 2360w, 1671s, 1609w, 1507w, 1312m, 1203w, 1155m, 973m, 818w.

[Mg(FTolP)$_2$(tmeda)] (4). Dibutylmagnesium (0.85 cm^3, 0.85 mmol) was added dropwise to a colourless solution of HFTolP (0.39 g, 1.74 mmol) and TMEDA (0.25 cm^3, 1.66 mmol) in toluene (40 cm^3). Stirring the clear colourless reaction mixture for *ca.* 30 min yielded a white precipitate. This was filtered and the filtrate concentrated *in vacuo*. Cooling to −30 °C resulted in the deposition of large colourless blocks of the title compound (0.37 g, 74%), m.p. 315 °C (dec.). ^{1}H NMR (C_6D_6, 300 K): δ 1.76 (s, 4H, NCH_2 tmeda), 1.99 (s, 12H, NCH_3 tmeda), 2.21 (s, 12H, Ar–CH_3), 6.92–7.04 (m, 16H, Ar-H), 8.55 (s, 2H, NCHN). ^{13}C NMR (C_6D_6, 300 K): δ 21.1 (s, Ar–CH_3), 46.8 (s, NCH_3 tmeda), 56.5 (s, NCH_2 tmeda), 121.2, 129.9, 131.2, 142.1 (s, Ar-C), 162.1 (s, NCHN). IR (Nujol) ν/cm^{-1}: 1886w, 1671w, 1568w, 1546m, 1500s, 1310s, 1293s, 1224m, 1172w, 1110m, 1062w, 1045w, 1016m, 979w, 953m, 826m, 813m, 801m, 773w, 644w, 588w.

[(μ_5-O)Li$_2$Zn$_3$\{(*p*-tolyl)NC(H)N(O)(*p*-tolyl)\}$_6$] (5). n-Butyllithium (1.1 cm^3, 2.2 mmol) was added dropwise to a colourless solution of HFTolP (0.5 g, 2.23 mmol) in diethyl ether (20 cm^3), yielding a clear yellow solution. This was stirred for *ca.* 1 h prior to dropwise addition to a static solution of anhydrous zinc chloride (0.15 g, 1.1 mmol), also in diethyl ether (20 cm^3). Standing at ambient temperature resulted in the deposition of a small quantity of colourless prisms (< 50 mg). An X-ray diffraction study identified these as the title compound. There was insufficient material for further spectroscopic or spectrometric characterisation.

[(μ_4-O)Zn$_4$(FTolP)$_6$] (6). *Method (i).* Diethylzinc (1.5 cm^3, 1.5 mmol) was added dropwise to a colourless solution of HFTolP (0.64 g, 2.85 mmol) in THF (40 cm^3), yielding a pale yellow opaque reaction mixture. After standing for *ca.* 30 min, the formation of small colourless crystals, suitable for an X-ray diffraction study, became evident. The mixture was filtered, concentrated slightly *in vacuo* and allowed to stand, whereupon a fine precipitate of the title compound deposited (0.13 g, 21%), m.p. > 325 °C.

Method (ii). A solution of HFTolP (0.45 g, 2.01 mmol), zinc acetate dihydrate (0.29 g, 1.32 mmol) and triethylamine (1.0 cm^3, 7.17 mmol) in methanol (50 cm^3) was refluxed at 70 °C for *ca.* 12 h. The resulting colourless precipitate was collected by filtration, dried *in vacuo*, washed with diethyl ether (3×10 cm^3) and dried by heating (*ca.* 60 °C) *in vacuo*. This yielded the solvent-free title compound as a free-flowing powder in moderate yield (*ca.* 60%). Subsequent recrystallisation from warm THF gave colourless prisms that were characterised as **6** by ^{1}H NMR and XRD (0.28 g, 52%), m.p. > 300 °C. ^{1}H NMR ($CDCl_3$, 300 K): δ 2.25 (s, 18H, Ar–CH_3), 2.31 (s, 18H, Ar–CH_3), 6.27 (m, 24H, Ar-H), 6.75 (m, 24H, Ar-H), 7.71 (br s, 6H, NCHN). ^{13}C NMR ($CDCl_3$, 300 K): δ 20.8 (s, Ar–CH_3), 123.0, 129.8, 131.8, 147.4 (s, Ar-C), 166.5 (s, NCHN). IR (Nujol) ν/cm^{-1}: 1543s, 1502m, 1331m, 1260m, 1229m, 1076m, 1018m, 979w, 928w, 816m.

X-Ray crystallography

Crystalline samples of compounds **1** and **3**–**6** were mounted in 0.5 mm capillaries and sealed under argon at ambient temperature. A crystalline sample of **2** was mounted upon a glass fibre in silicone grease at −150 °C (123 K). Crystal data for compounds **1** and **3**–**6** were obtained using a Bruker SMART CCD diffractometer. Data for **2** were obtained on an Enraf-Nonius Kappa CCD instrument. Data was corrected for absorption using the SADABS program.[53] Structural solution and refinement was carried out using SHELXL-97[54] and SHELXS-97,[55] utilising the graphical interface X-Seed.[56] All non-hydrogen atoms were located and were refined with anisotropic thermal parameters. Hydrogen atoms were placed in calculated positions (riding model) and were not refined. Compound **5** suffered from disorder in the phenyl rings. This

disorder was reasonably well modelled, with all aromatic rings having idealised geometry, however, the final *r*-factor was still quite high. There is, however, no ambiguity about the connectivity of the structure. Data for compound **6** were rather weak leading to a higher residuals than might be expected for this type of complex. Crystal data and refinement parameters for all complexes are compiled in Table 1.

CCDC reference numbers 185261–185266. See http://www.rsc.org/suppdata/nj/b2/b204304a/ for crystallographic data in CIF or other electronic format.

Acknowledgements

The authors gratefully acknowledge the continued financial support of the Australian Research Council (RIEFP grant for Bruker SMART CCD X-ray diffractometer). M. L. C. would like to acknowledge the Royal Society, UK, for the provision of a postdoctoral fellowship.

References and notes

1 J. Barker and M. Kilner, *Coord. Chem. Rev.*, 1994, **133**, 219.
2 F. T. Edelmann, *Coord. Chem. Rev.*, 1994, **137**, 403.
3 F. A. Cotton, L. M. Daniels and C. A. Murillo, *Inorg. Chem.*, 1993, **32**, 2881.
4 J. A. R. Schmidt and J. Arnold, *Chem. Commun.*, 1999, 2149.
5 K. Kincaid, C. P. Gerlach, G. R. Giesbrecht, J. R. Hagadorn, G. D. Whitener, A. Shafir and J. Arnold, *Organometallics*, 1999, **18**, 5360.
6 M. P. Coles and R. F. Jordan, *J. Am. Chem. Soc.*, 1997, **119**, 8125.
7 G. D. Whitener, J. Hagadorn and J. Arnold, *J. Chem. Soc., Dalton Trans.*, 1999, 1249.
8 D. Abeysekera, K. N. Robertson, T. S. Cameron and J. A. C. Clyburne, *Organometallics*, 2001, **20**, 5532.
9 M. P. Coles, D. C. Swenson, R. F. Jordan and V. G. Young, Jr., *Organometallics*, 1997, **16**, 5183.
10 S. Dagorne, I. A. Guzei, M. P. Coles and R. F. Jordan, *J. Am. Chem. Soc.*, 2000, **122**, 274.
11 G. Talarico and P. H. M. Budzelaar, *Organometallics*, 2000, **19**, 5691.
12 A. R. Kennedy, R. E. Mulvey and R. B. Rowlings, *J. Am. Chem. Soc.*, 1998, **120**, 7816.
13 Y. Zhou and D. S. Richeson, *Inorg. Chem.*, 1996, **35**, 2448.
14 Y. Zhou and D. S. Richeson, *Inorg. Chem.*, 1997, **36**, 501.
15 S. Dagorne, R. F. Jordan and V. G. Young, Jr., *Organometallics*, 1999, **18**, 4619.
16 S. R. Foley, Y. Zhou, G. P. A. Yap and D. S. Richeson, *Inorg. Chem.*, 2000, **39**, 924.
17 F. A. Cotton, L. M. Daniels, L. R. Falvello and C. A. Murillo, *Inorg. Chim. Acta*, 1994, **219**, 7.
18 F. A. Cotton, L. M. Daniels, D. J. Maloney and C. A. Murillo, *Inorg. Chim. Acta*, 1996, **249**, 9.
19 F. A. Cotton, L. M. Daniels, L. R. Falvello, J. H. Matonic, C. A. Murillo, X. Wang and H. Zhou, *Inorg. Chim. Acta.*, 1997, **266**, 91.
20 F. A. Cotton, S. C. Haefner, J. H. Matonic, X. Wang and C. A. Murillo, *Polyhedron*, 1997, **16**, 541.
21 D. M. Grove, G. van Koten, H. J. C. Ubbels, K. Vrieze, L. C. Niemann and C. H. Stam, *J. Chem. Soc., Dalton Trans.*, 1986, 717.
22 J. Barker, K. Milner and R. O. Gould, *J. Chem. Soc., Dalton Trans.*, 1987, 2687.
23 M. G. B. Drew and J. D. Wilkins, *J. Chem. Soc., Dalton Trans.*, 1974, 1973.
24 F. A. Cotton, T. Inglis, M. Kilner and T. R. Webb, *Inorg. Chem.*, 1975, **14**, 2023.
25 N. G. Connelly, P. M. Hopkins, A. G. Orpen, G. M. Rosair and F. Viguri, *J. Chem. Soc., Dalton Trans.*, 1992, 2907.
26 P. B. Hitchcock, M. F. Lappert and D.-S. Liu, *J. Organomet. Chem.*, 1995, **488**, 241.
27 P. B. Hitchcock, M. F. Lappert and M. Layh, *J. Chem. Soc., Dalton Trans.*, 1998, 3113.
28 G. R. Giesbrecht, A. Shaffir and J. Arnold, *J. Chem. Soc., Dalton Trans.*, 1999, 3601.
29 P. C. Junk and L. M. Louis, unpublished results.
30 C.-F. Lee, K.-F. Chin, S.-M. Peng and C.-M. Che, *J. Chem. Soc., Dalton Trans.*, 1993, 467.
31 A. R. Saddique, M. J. Hegg and C. H. Winter, *Inorg. Chem.*, 2001, **40**, 6349.
32 M. Westerhausen and H.-D. Hausen, *Z. Anorg. Allg. Chem.*, 1992, **27**, 615.
33 D. Walther, P. Gebhardt, R. Fischer, U. Kreher and H. Gorls, *Inorg. Chim. Acta*, 1998, **281**, 181.
34 B. Srinvas, C.-C. Chang, C.-H. Chen, M. Y. Chiang, I.-T. Chen, Y. Wang and G.-H. Lee, *J. Chem. Soc., Dalton Trans.*, 1997, 957.
35 Obtained from a survey of the Cambridge Crystallographic Structural Database.
36 S.-G. Roh, A. Proust, P. Gouzerh and F. Robert, *J. Chem. Soc., Chem. Commun.*, 1993, 836.
37 R. P. Davies, D. J. Linton, R. Snaith and A. E. H. Wheatley, *Chem. Commun.*, 2000, 1819.
38 A. D. Bond, D. J. Linton, P. Schooler and A. E. H. Wheatley, *J. Chem. Soc., Dalton Trans.*, 2001, 3173.
39 M. Uchiyama, M. Koike, M. Kameda, Y. Kondo and T. Sakamoto, *J. Am. Chem. Soc.*, 1996, **118**, 8733.
40 M. Uchiyama, M. Kameda, O. Mishima, N. Yokoyama, M. Koike, Y. Kondo and T. Sakamoto, *J. Am. Chem. Soc.*, 1998, **120**, 4934.
41 M. F. Lappert, P. P. Power, A. R. Sanger, R. C. Srivastava, *Metal and Metalloid Amides*, Ellis Horwood Ltd., Chichester, 1980.
42 T. G. Wetzel and P. W. Roesky, *Z. Anorg. Allg. Chem.*, 1999, **625**, 1953.
43 T. Chivers, A. Downard and M. Parvez, *Inorg. Chem.*, 1999, **38**, 4347.
44 A. Tulinsky, C. R. Worthington and E. Pignataro, *Acta Crystallogr.*, 1959, **12**, 623.
45 A. Tulinsky and C. R. Worthington, *Acta Crystallogr.*, 1959, **12**, 626.
46 A. Tulinsky, *Acta Crystallogr.*, 1959, **12**, 634.
47 L. Hiltunen, M. Leskelä, M. Mäkelä and L. Niinistö, *Acta Chem. Scand. Ser. A*, 1987, **41**, 548.
48 W. Clegg, D. R. Harbron, C. D. Homan, P. A. Hunt, I. R. Little and B. P. Straughan, *Inorg. Chim. Acta*, 1991, **186**, 51.
49 A. Belforte, F. Calderazzo, U. Englert and J. Strähle, *Inorg. Chem.*, 1991, **30**, 3778.
50 A. Kasani, R. P. Kamalesh Babu, K. Feghali, S. Gambarotta, G. P. A. Yap, L. K. Thompson and R. Herbst-Irmer, *Chem. Eur. J.*, 1999, **5**, 577.
51 M. Corbett and B. F. Hoskins, *Inorg. Nucl. Chem. Lett.*, 1970, **6**, 261.
52 R. M. Roberts, *J. Org. Chem.*, 1949, **14**, 277.
53 R. H. Blessing, *Acta Crystallogr., Sect. A.*, 1995, **51**, 33.
54 G. M. Sheldrick, SHELXL-97, University of Göttingen, Germany, 1997.
55 G. M. Sheldrick, SHELXS-97, University of Göttingen, Germany, 1997.
56 L. J. Barbour, X-Seed, Crystallographic Interface, University of Missouri-Columbia, USA, 1999.